In situ spectroscopic identification of the six types of asbestos

Vladimir Zholobenko [a]*, Frank Rutten [a,b], Aleksey Zholobenko [c], Amy Holmes [a]

[a] *School of Chemical and Physical Sciences, Keele University, Keele, ST5 5BG, United Kingdom*

[b] *ATBC, HAN University of Applied Sciences, 6525 EM Nijmegen, The Netherlands*

[c] *Larchwood, Newcastle-under-Lyme, ST5 5BB, United Kingdom*

Supporting Information

Contents

* Corresponding author, e-mail address: v.l.zholobenko@keele.ac.uk

1. Experimental Procedures

Table S1. Samples analysed using FTIR and Raman spectroscopy.

Asbestos	Matrix Materials
chrysotile	quartz wool
amosite	glass wool
crocidolite	mineral wool
actinolite	nylon
anthophyllite	bitumen
tremolite	plaster
	cement
	plasterboard
	calcium carbonate
	floor tile
	stone
	pvc plastic
	ceramic tile
	terracotta brick
	rubber belt
	wood block
	clay brick

2. Results and Discussion

2.1. FTIR Data

Six types of geological asbestos reference samples have been studied (chrysotile, crocidolite, amosite, tremolite, anthophyllite and actinolite). Figure S1 shows characteristic spectra of these materials. The 3700-3500 cm^{-1} region can be attributed to O-H stretching vibrations, whereas the bands observed in the 1200-500 cm^{-1} region can be attributed to various lattice vibrations (Table S2). The mid-IR spectra of chrysotile are quite different from those of amphiboles. The latter demonstrate a number of similar features, e.g. both crocidolite and amosite are iron rich, and hence the bands related to the Fe-O and FeOH vibrations are observed for both samples. However, alterations in the chemical composition within each sample lead to different bonding, and hence changes in the band position.

Table S2. Key bands in FTIR spectra of reference asbestos samples and their assignment (Ref [1,2,3,4,5,6,7]; band position in cm^{-1})

Chrysotile	Actinolite	Amosite	Anthophyllite	Crocidolite	Tremolite	Assignment
3683	3673	3653	3674	3650	3674	ν(O-H)
3643	3659	3637	3658	3635	3660	
	3643	3618		3619		
1069	1080	1128		1143	1105	ν_{as}(Si-O-Si)
	1035	1079	1070	1098	1071	
942	985	991	1007	986	990	non-bridging
	942	952	925	971	946	ν(O-Si^-)
	913	882	857		920	
	755	773		775	876	ν_s(Si-O-Si)
		730	724	724	757	ν(M-O)
602	682	699	668	689	684	and
	657	629		655	662	ŭ(M-OH)
	641	530	563	630	533	ŭ(Si-O-Si)

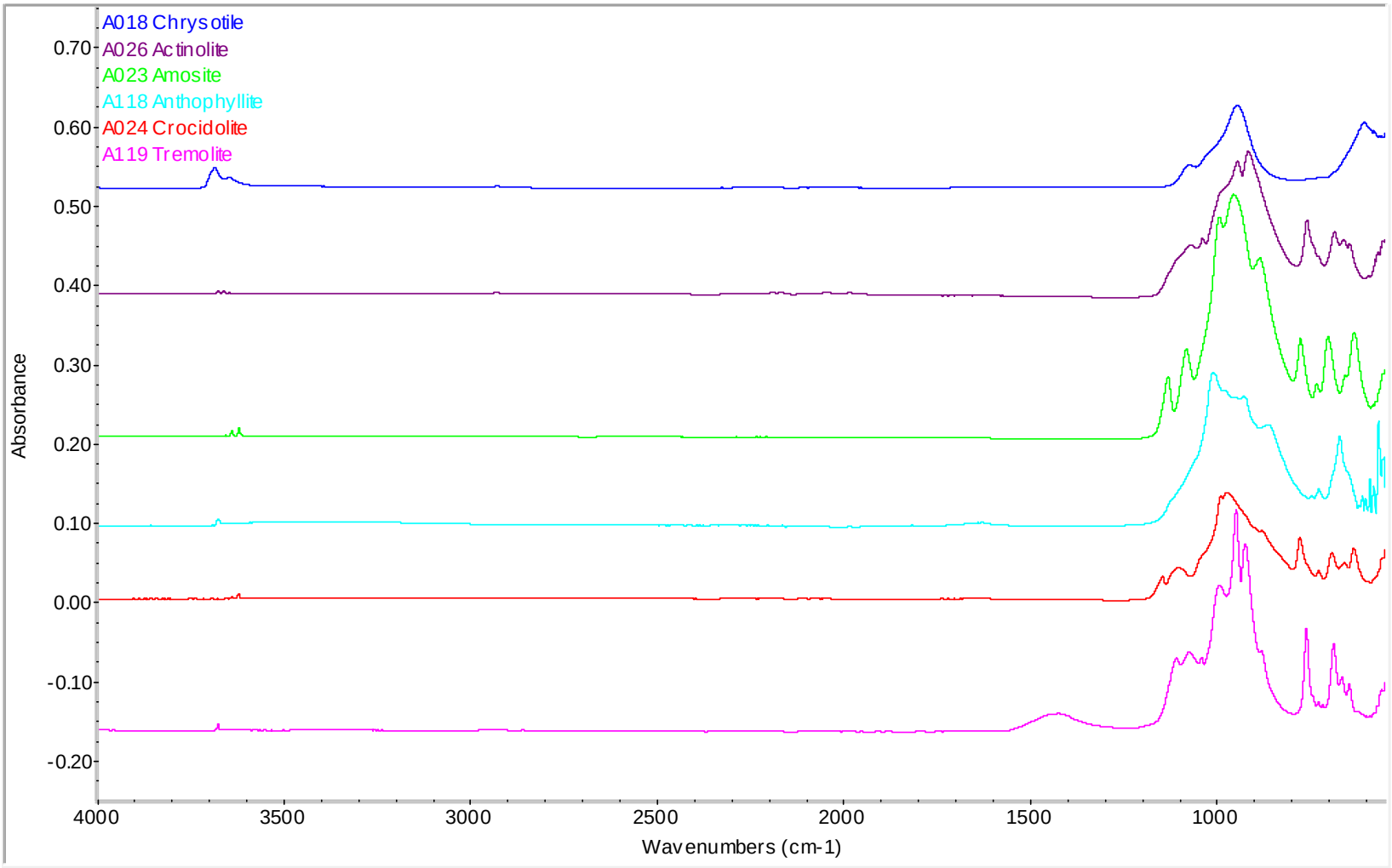

Figure S1. Wide range FTIR spectra of the reference asbestos samples.

49

There is a wide range of materials which could be found in combination with asbestos or as its substitutes, including asbestos replacement fibres and matrix materials. FTIR spectra of the possible replacement fibres are shown in Figure S2. The silica-based inorganic fibres, e.g. glass wool, show intense bands in the 1200-900 cm^{-1} region, which can be assigned to ν_{as}(Si-O-Si) and ν_{as}(O-Si-O) vibrations. The organic fibre, nylon, shows a very different spectrum, with bands in the 3400-2800 and 1700-700 cm^{-1} regions. The bands between 3400-2800 cm^{-1} can be attributed to ν(N-H) and ν(C-H) and the bands between 1700-700 cm^{-1} can be attributed to ν(C-C), ν(C=O), δ(C-H) and ν(C-O) vibrations.

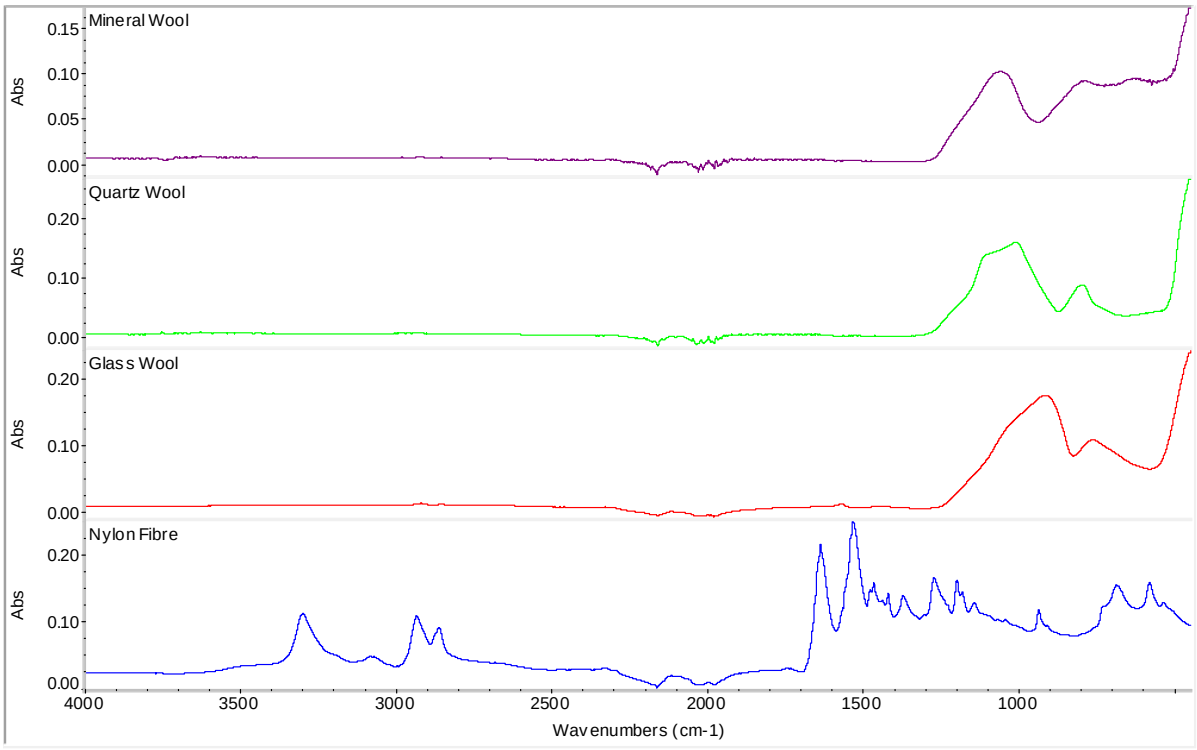

Figure S2. Spectra of potential asbestos replacement fibres.

Figure S3 shows FTIR spectra of three common matrix materials. Bitumen is a mixture of phenolic resins commonly used in industry to encapsulate various materials, including asbestos. The FTIR spectra show bands in the 3000-2800 cm^{-1} region which can be attributed to ɜ(C-H). Bands in the 1600-1300 cm^{-1} region can be ascribed to ŭ(CH_2), ŭ(CH_3) and ɜ(C=C). Two potential inorganic matrix materials have been also considered. Cement is a mixture of calcium silicate hydrate, calcium sulphate and calcium carbonate. The broad band at 1400 cm^{-1} can be attributed to the calcium carbonate component, in particular the C-O stretching vibrations. All three components contribute to the bands observed at lower wavenumbers. Plasterboard is also a composite material, comprising calcium sulphate, calcium carbonate and cellulose as well as other filler materials. Bands observed in the 3600-3400 cm^{-1} region could be attributed to various O-H stretching vibrations.

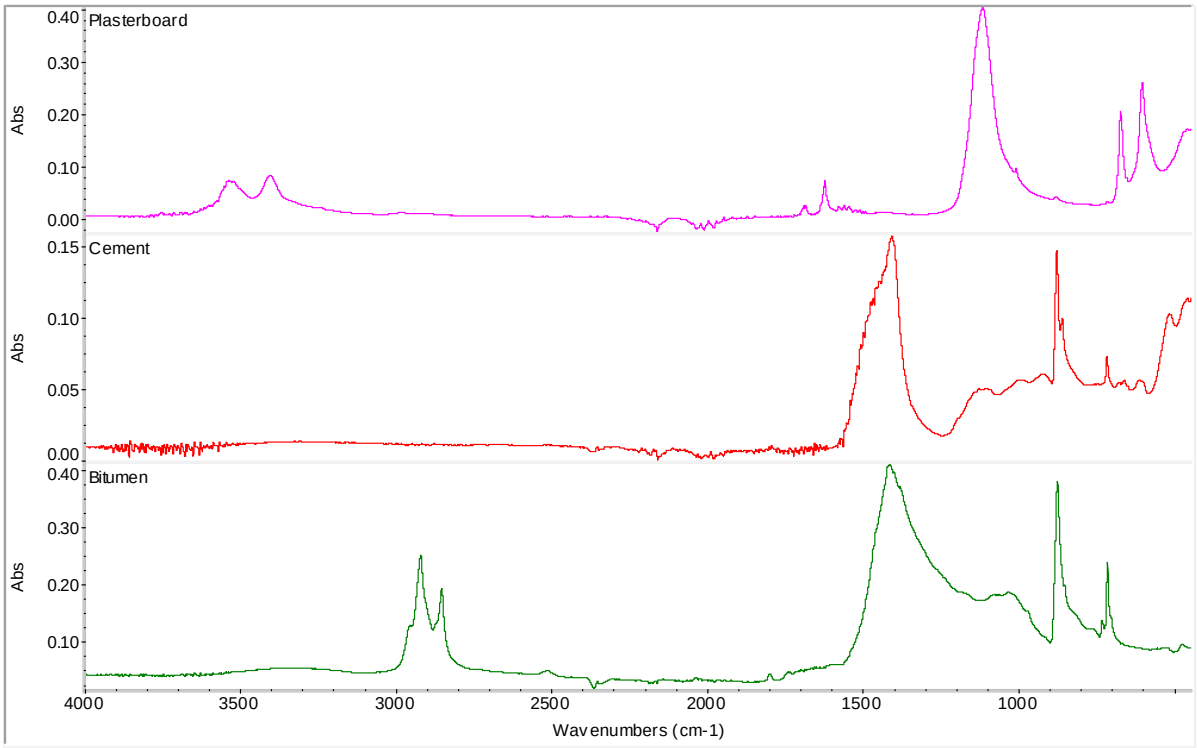

Figure S3. Spectra of potential asbestos matrix materials.

FTIR analyses of materials with unknown asbestos content

Figure 4 shows spectra of samples 32, 35 and 14 along with the reference spectra for chrysotile and amosite. The spectrum of sample 32 shows a few bands in common with the chrysotile spectra, e.g. the ɜ(O-H) at 3700-3600 cm^{-1}. The bands at lower wavenumbers are partially obscured by other components of the sample but can still be clearly identified.

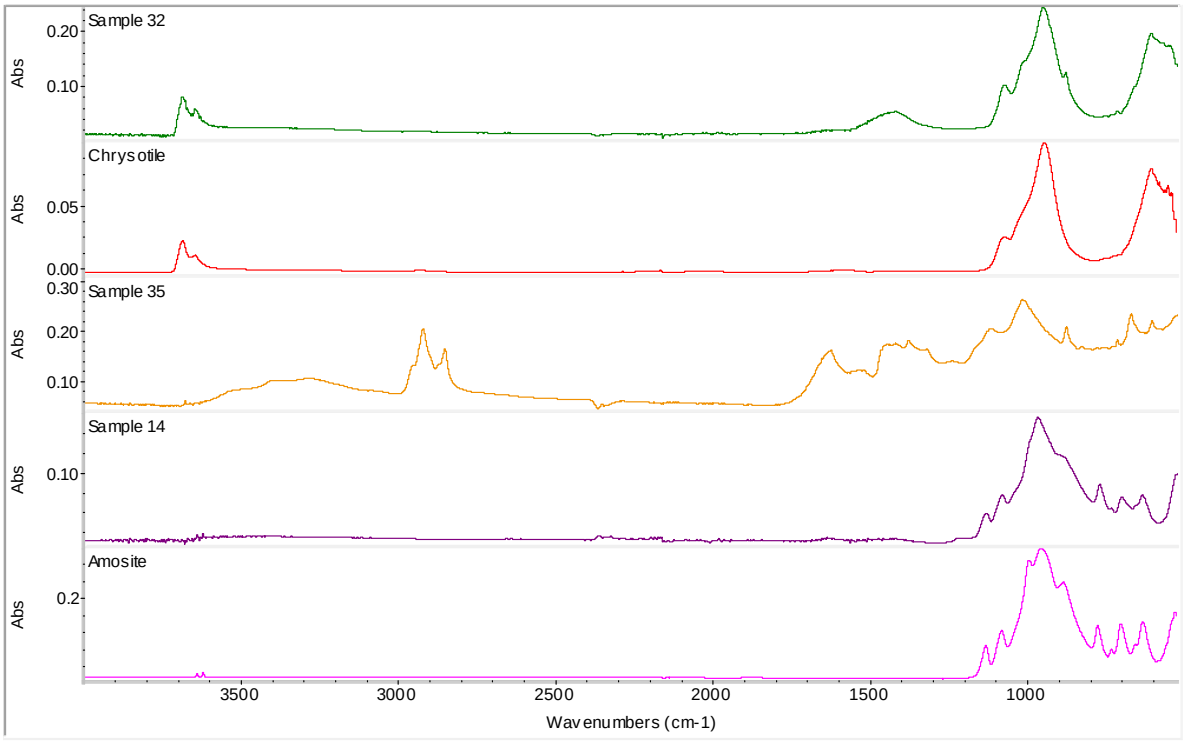

Figure S4. FTIR spectra of samples 32, 35 and 14, along with reference chrysotile and amosite.

For sample 35 the distinctive ɜ(O-H) chrysotile bands in the 3700-3600 cm^{-1} region have not been observed. The bands in the 1500-500 cm^{-1} region, which would be expected for asbestos, cannot be accurately attributed to an asbestos type, and overall, there is not enough information to determine whether asbestos is present. This could have been due to the asbestos fibres being encased in the matrix material, and hence not detected. The spectrum of sample 14 shows bands in the 1200-400 cm^{-1} region, which can be clearly attributed to amosite, the ɜ(O-H) bands at 3700-3600 cm^{-1} which are indicative of chrysotile are not observed, despite PLM indicating the presence of this type of asbestos. Although this qualitative approach can work for ñeasyò samples with a high asbestos content, the potential of FTIR analysis has been explored using a specialised software package Specta, which is designed for the identification of individual components in mixed samples using reference libraries containing infrared spectra of reference asbestos and matrix materials. For each

of the 43 samples considered, the results obtained by Specta have been compared to those obtained by PLM.

In Figure S5, the match value for sample 32, at 80.06, shows good agreement between the sample and composite spectra in terms of both band position and intensity. The sample contains a mixture of cement and asbestos, which has been identified as chrysotile by PLM. Specta used four reference spectra to produce the composite spectrum, two for chrysotile (~50%), one for cement (~42%) and one for crocidolite (~8%). The presence of cement and chrysotile has been correctly identified using Specta. Crocidolite has not been detected using PLM, but it is possible that it is present at a low concentration, and hence not detected, or that Specta simulation gives a false positive due to the overlap of bands in the 1100-800 cm^{-1} range.

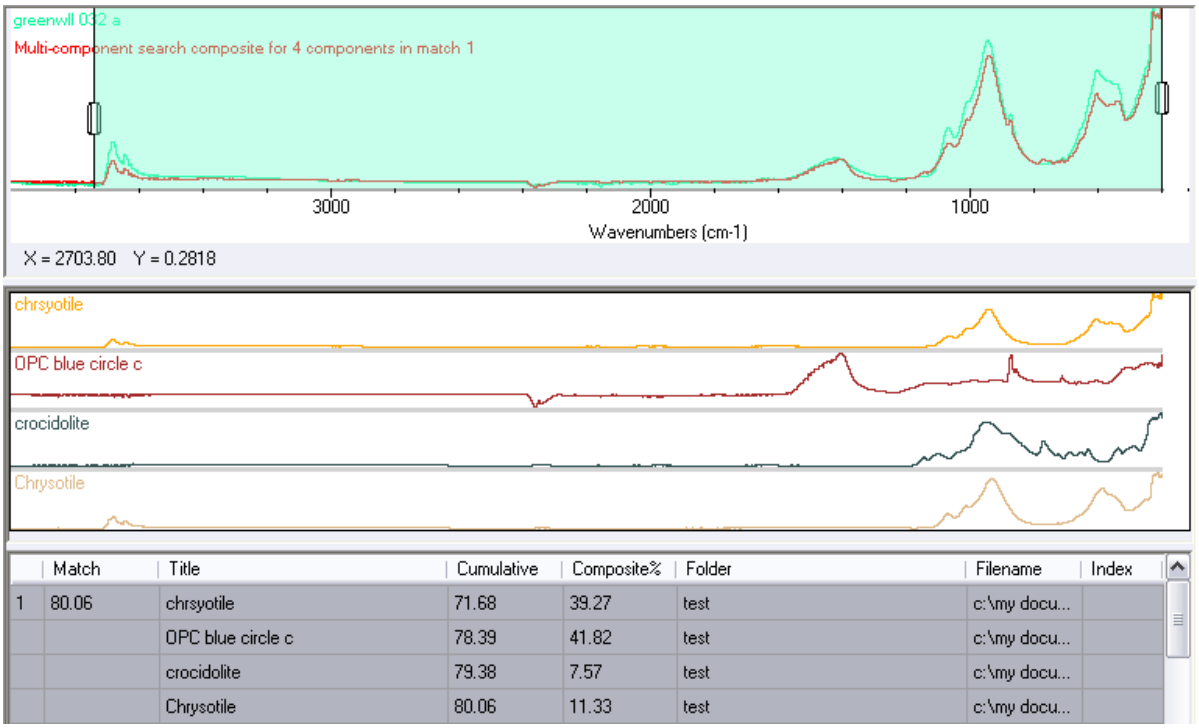

	Match	Title	Cumulative	Composite%	Folder	Filename	Index
1	80.06	chrsyotile	71.68	39.27	test	c:\my docu...	
		OPC blue circle c	78.39	41.82	test	c:\my docu...	
		crocidolite	79.38	7.57	test	c:\my docu...	
		Chrysotile	80.06	11.33	test	c:\my docu...	

Figure S5. Sample 32 ï FTIR spectrum, composite spectrum and chrysotile, OPC and crocidolite reference spectra.

For sample 35 and its simulated composite spectrum, the match value is 64.47 showing very similar band positions in the two spectra, however, there are noticeable differences in the band intensities (Figure S6). The sample is roof felt, and PLM could not determine whether or not asbestos was present in the sample. Specta results indicate that no asbestos is present in the sample, with the four reference components being poly(ethylene-propylene-diene) (~10%), plasterboard (~26%), tile (~41%) and cement (~23%). While the match value indicates with reasonable certainty

that there is no asbestos present, a confident determination of the sample composition is hardly possible. This exposes a significant problem with using the Specta software for the analysis of real-life samples, if unknown components of the sample are not in the reference library, a good match cannot be obtained.

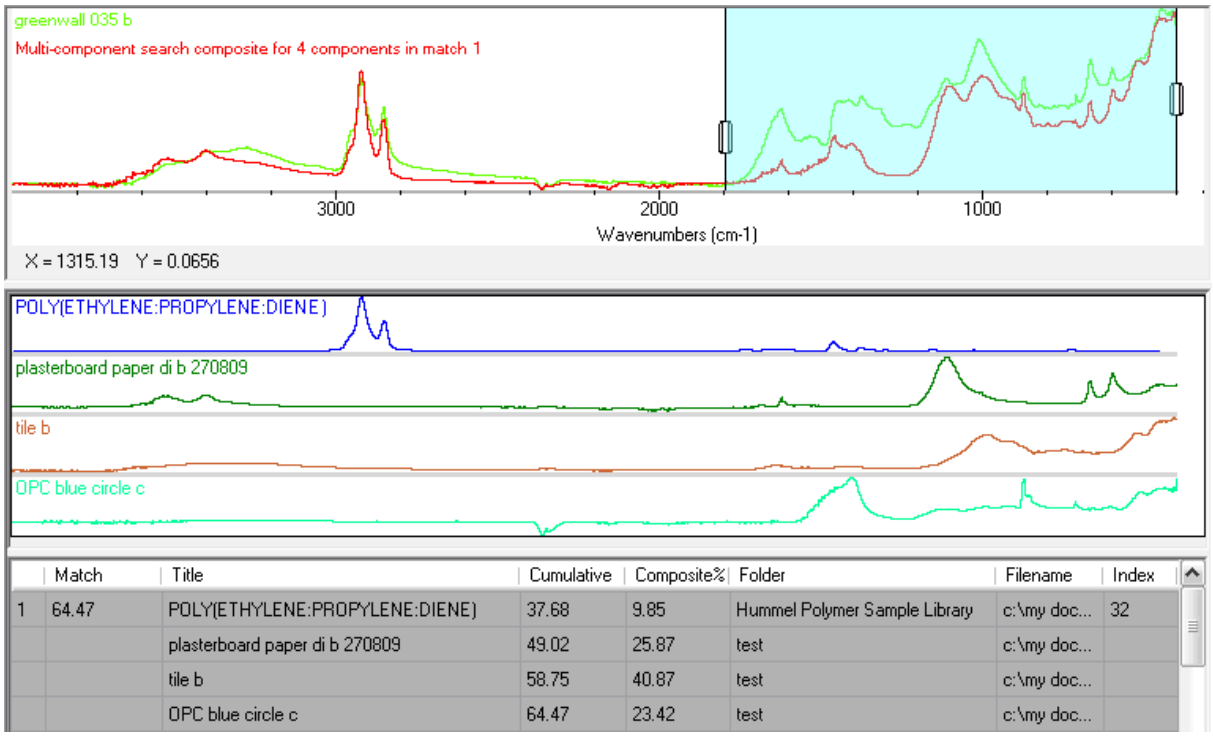

	Match	Title	Cumulative	Composite%	Folder	Filename	Index
1	64.47	POLY(ETHYLENE:PROPYLENE:DIENE)	37.68	9.85	Hummel Polymer Sample Library	c:\my doc...	32
		plasterboard paper di b 270809	49.02	25.87	test	c:\my doc...	
		tile b	58.75	40.87	test	c:\my doc...	
		OPC blue circle c	64.47	23.42	test	c:\my doc...	

Figure S6. Sample 35 ï FTIR spectrum, composite spectrum and poly(ethylene-propylene-diene), plasterboard, tile and cement reference spectra.

Table S3 summarises the results of PLM and FTIR analyses demonstrating good agreement between the two techniques for 34 out 43 samples. For a number of challenging materials, neither PLM nor FTIR analysis provided definitive confirmation of the asbestos presence.

120 Table S3. Samples suspected to contain asbestos: PLM and FTIR results.

Sample	PLM	FTIR
1: red floor tile	chrysotile	chrysotile
2: black floor tile	chrysotile	chrysotile
3: cement	chrysotile	chrysotile
4: loft hatch	amosite + chrysotile	chrysotile
5: cement sheeting	chrysotile	chrysotile
6: board	chrysotile	no asbestos detected
7: black floor tile	chrysotile	chrysotile
8: beige floor tile	chrysotile	chrysotile
9: green floor tile	chrysotile	chrysotile
10: cream floor tile	chrysotile	chrysotile
11: cream floor tile	chrysotile	chrysotile
12: sink pad	chrysotile	chrysotile
13: cement	chrysotile	chrysotile
14:cement board	amosite + chrysotile	amosite
15: insulation material	amosite + chrysotile	amosite
16: artex	no asbestos detected	no asbestos detected
17: step nosing	no asbestos detected	chrysotile
18: artex	no asbestos detected	no asbestos detected
19: roof cement	chrysotile	chrysotile
20: sink pad	no asbestos detected	no asbestos detected
21: roof felt	no asbestos detected	amosite
22: cream floor tile	no asbestos detected	no asbestos detected
23: cement	no asbestos detected	chrysotile
24: sink pad	no asbestos detected	no asbestos detected
25: sink pad	no asbestos detected	no asbestos detected
26: blue vinyl tile	no asbestos detected	no asbestos detected
27: red floor tile	chrysotile	chrysotile
28: black floor tile	chrysotile	chrysotile
29: cement	chrysotile	chrysotile
30: guttering cement	chrysotile	chrysotile
31: loft hatch	no asbestos detected	chrysotile
32: side moulding- cement	chrysotile	chrysotile+crocidolite
33: insulation material	no asbestos detected	amosite
34: door panel	amosite	amosite
35: roof felt	no asbestos detected	no asbestos detected
36: board	no asbestos detected	no asbestos detected
37: white material	no asbestos detected	no asbestos detected
38: black block	no asbestos detected	chrysotile
39: artex	no asbestos detected	no asbestos detected
40: black floor tile	no asbestos detected	no asbestos detected
41: board material	no asbestos detected	no asbestos detected
42: cement	no asbestos detected	no asbestos detected
43: asbestos rope	chrysotile	chrysotile

121

122

2.2. Raman Spectroscopy

Raman spectra of the reference materials and a selection of ACM have been collected using different excitation laser wavelengths (Figures S7 and S8), and the band positions are summarised in Table S4. The data are in good agreement with those reported in the literature [8,9,10,11,12,13]. However, the signal to noise ratio is lower than that for FTIR and NIR spectra, and for some coloured materials the fluorescence background is relatively high. To the best of our knowledge, only one publication presented high quality data, with no fluorescence interference, obtained using 240-nm laser excitation [14], although some data in this reference disagree with the literature. It should also be noted that utilising such instrumentation would be impractical for in situ or on-site analysis.

Table S4. Key bands in the Raman spectra of reference asbestos samples and their assignment (band position in cm^{-1}).

Chrysotile	Actinolite	Amosite	Anthophyllite	Crocidolite	Tremolite	Assignment
1105	1048	1019	1043	964	1060	ν_{as}(Si-O-Si)
	1023	967			1029	
692	668	660	674		674	ν_{s}(Si-O-Si)
623						
		528	429	534		δ(Si-O-Si)
389	382	349	382		394	ν(M-O)
345			361		370	
232	217				223	ν(O-H-O)
129	172	181	192	166	178	
	147	154	112	143	123	lattice
	114	78	60	105		vibrations

Samples 32 and 43 were previously identified using FTIR and PLM as containing a high level of chrysotile. However, no indication of chrysotile presence has been provided by Raman spectroscopy, the bands observed for sample 32 can all be attributed to the calcium carbonate component of cement. Sample 43 also contains chrysotile, albeit at a lower concentration than in sample 32, which also has not been detected in the Raman spectra.

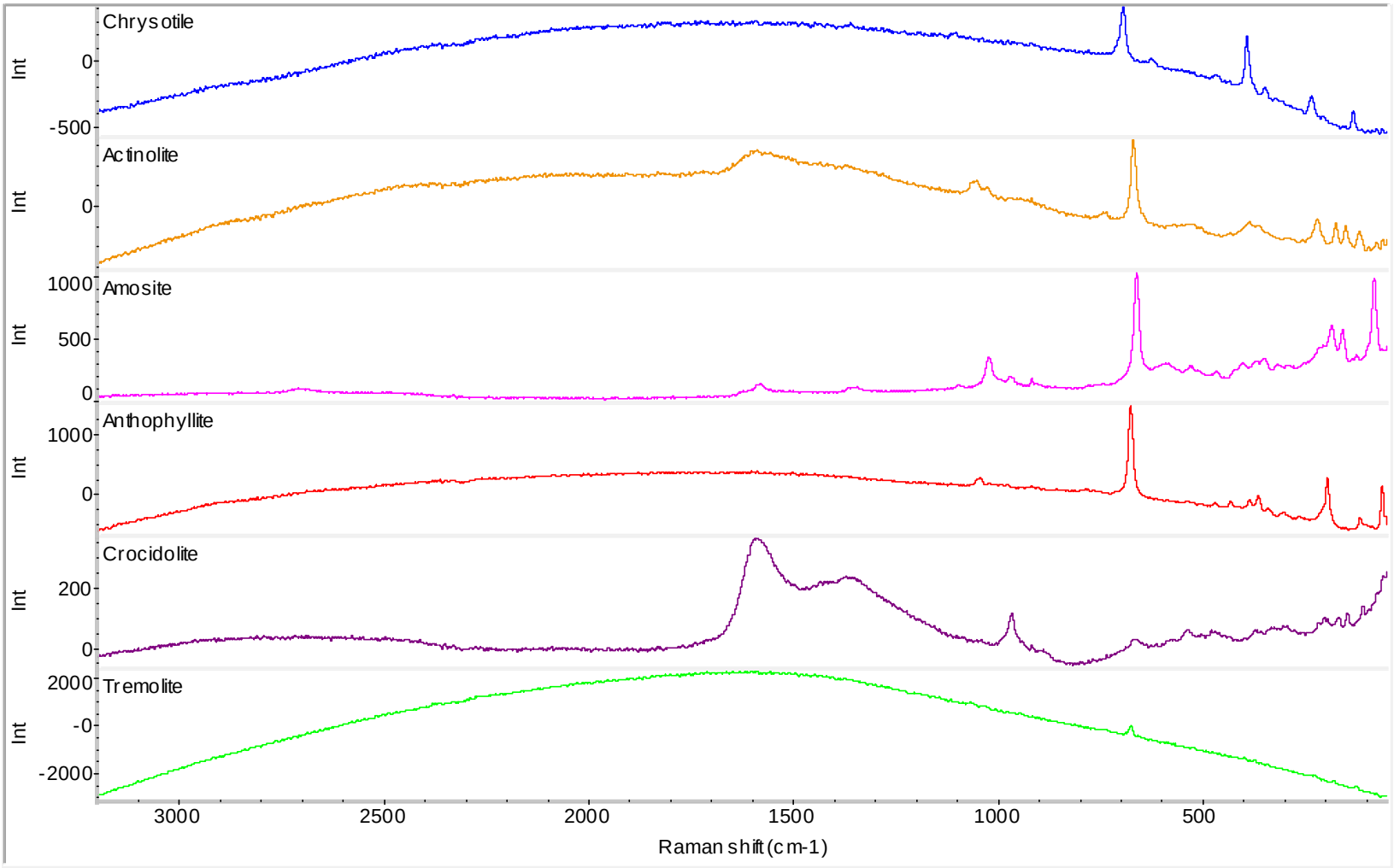

Figure S7a. Raman spectra of asbestos reference samples collected using 532 nm excitation wavelength.

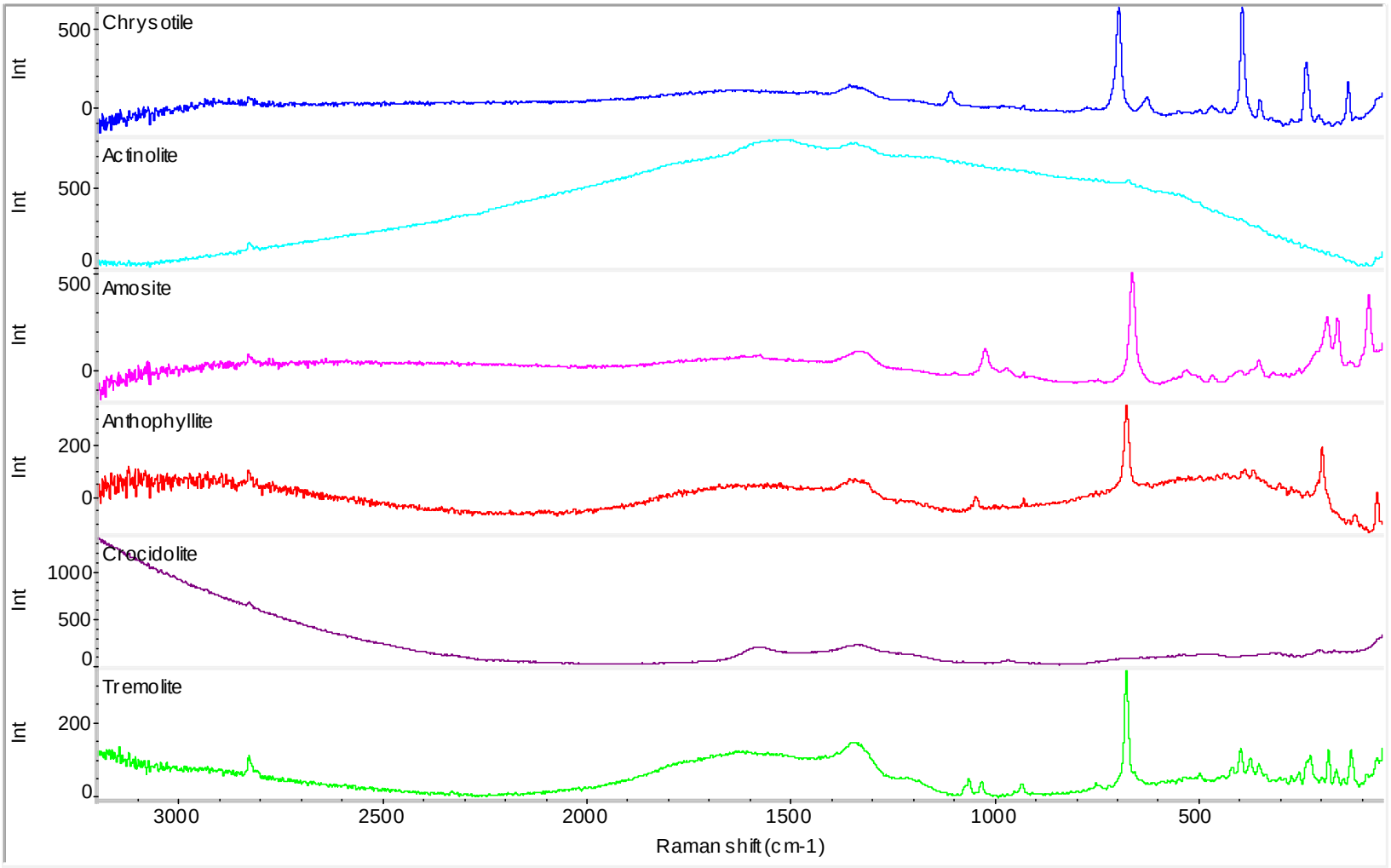

Figure S7b. Raman spectra of asbestos reference samples collected using 780 nm excitation wavelength.

145

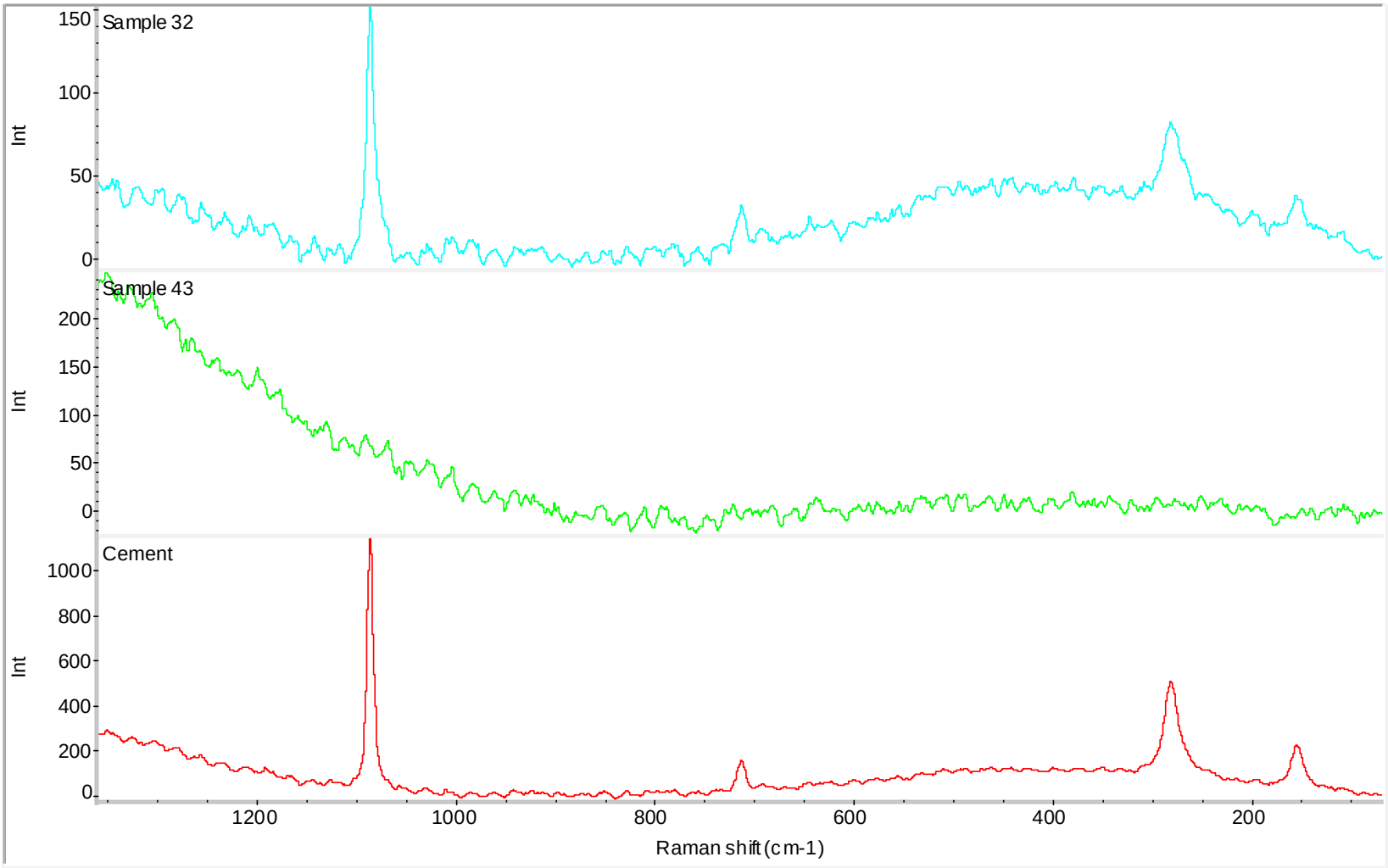

Figure S8. Raman spectra of samples 32 and 43 and of cement, collected using a 532 nm excitation laser source.

149 *2.3. Near-infrared spectroscopy.*

150 Figures S9 and S10 show NIR spectra of reference asbestos samples and of some matrix materials, collected at a 2 cm^{-1} resolution.

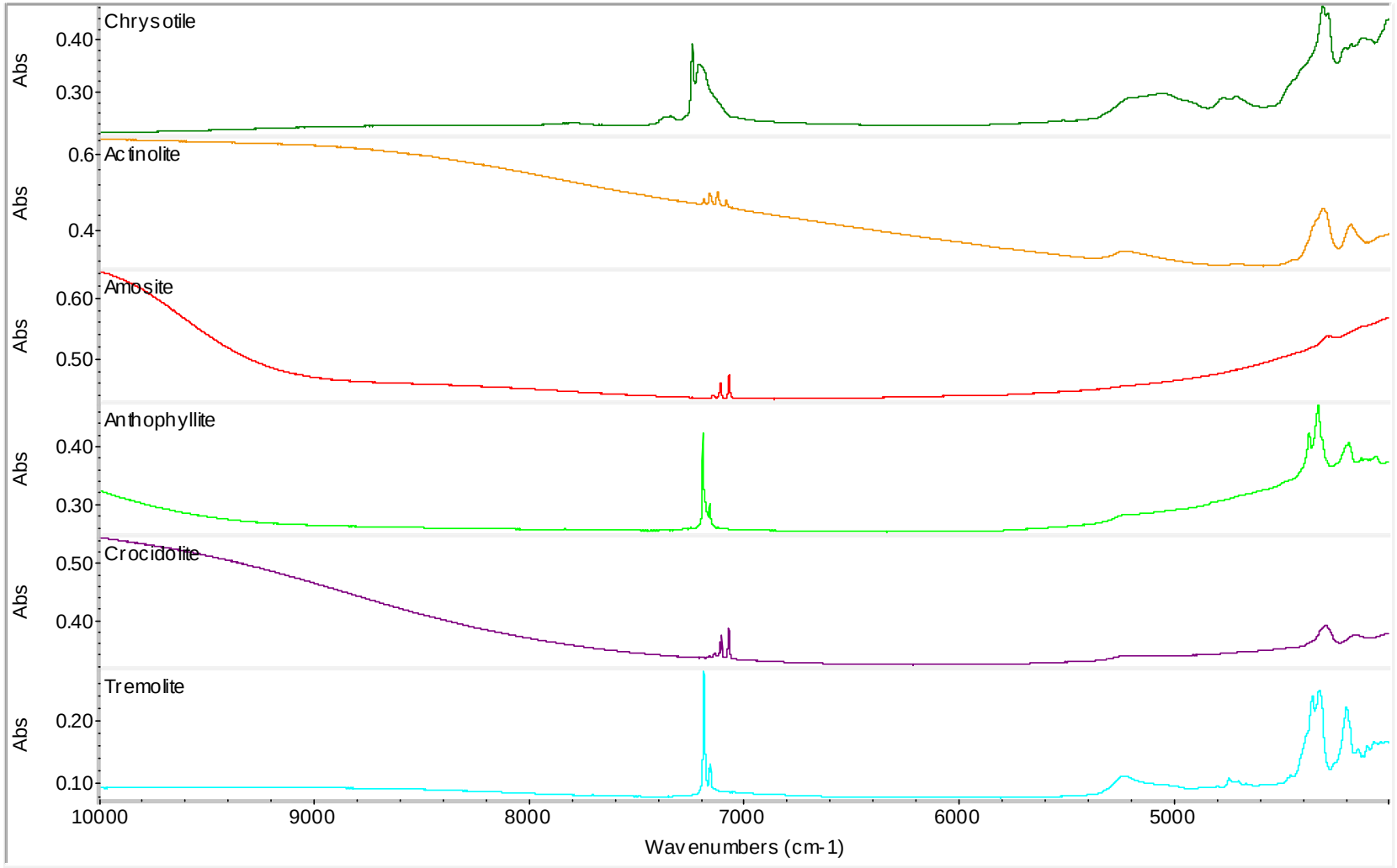

Figure S9a. Wide-range NIR spectra of asbestos reference samples (resolution = 2 cm^{-1}).

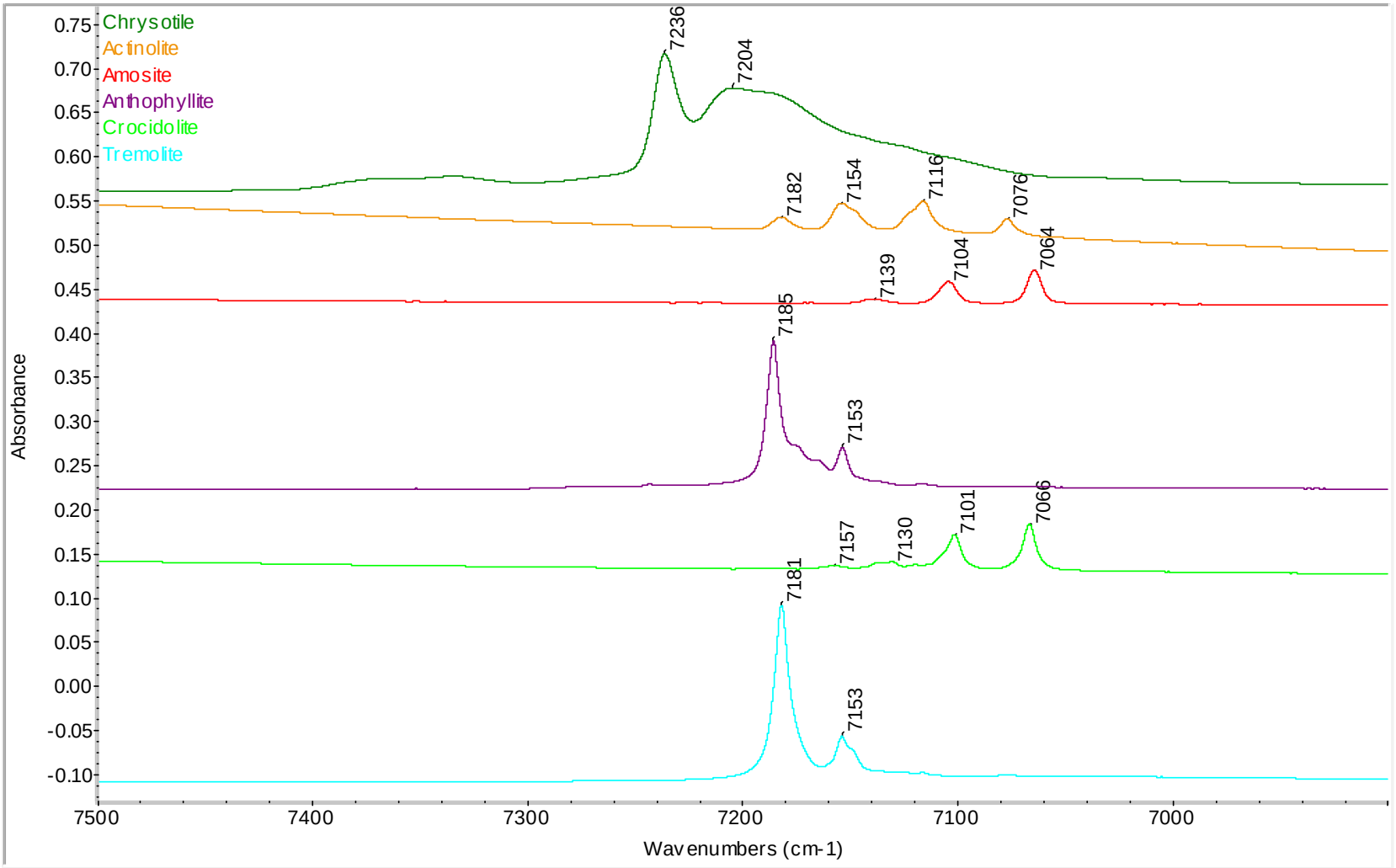

Figure S9b. NIR spectra of asbestos reference samples (first overtone of the O-H stretching vibrations; resolution = 2 cm^{-1}).

151

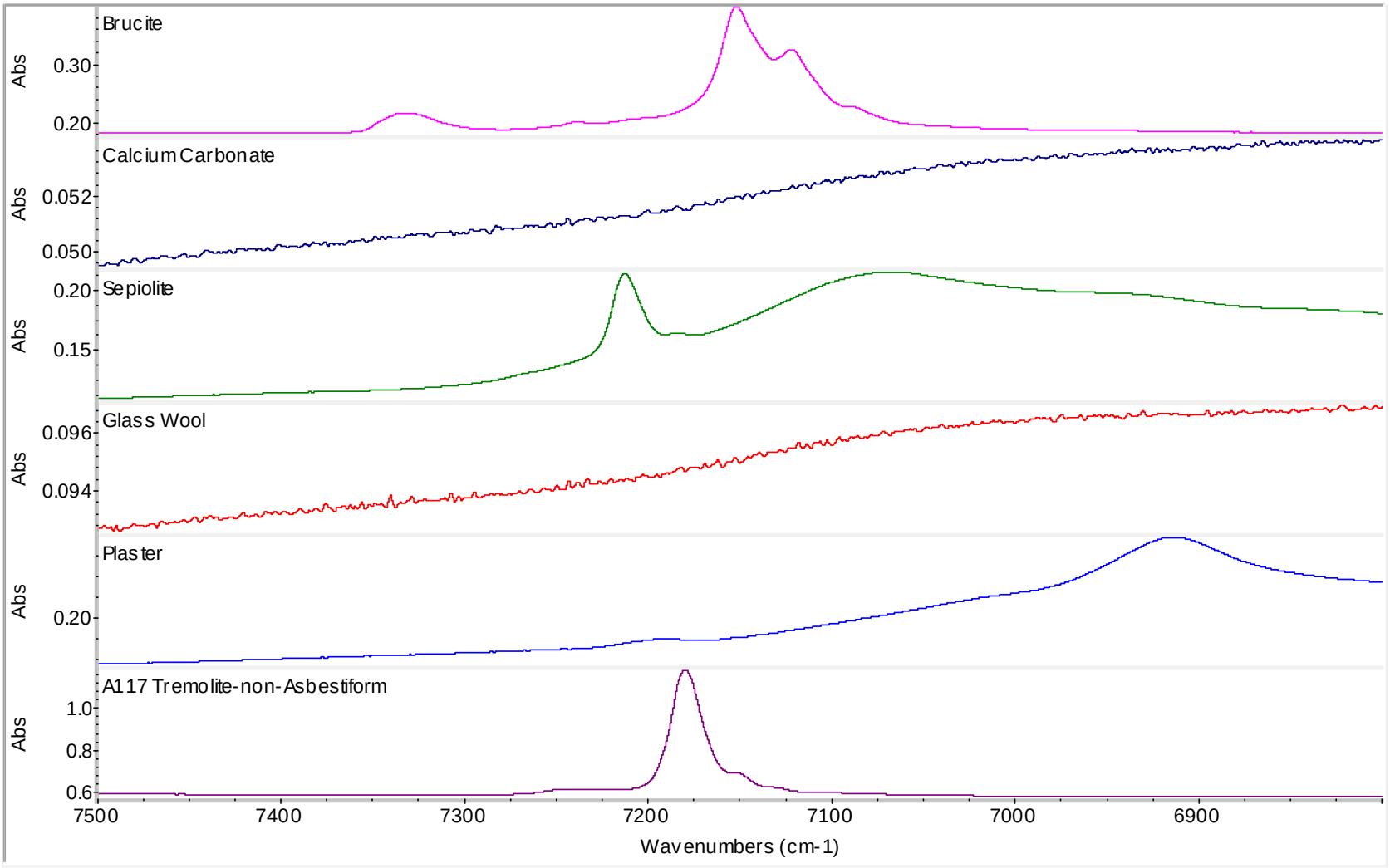

Figure S10. NIR spectra of reference matrix materials (resolution = 2 cm^{-1}).

152

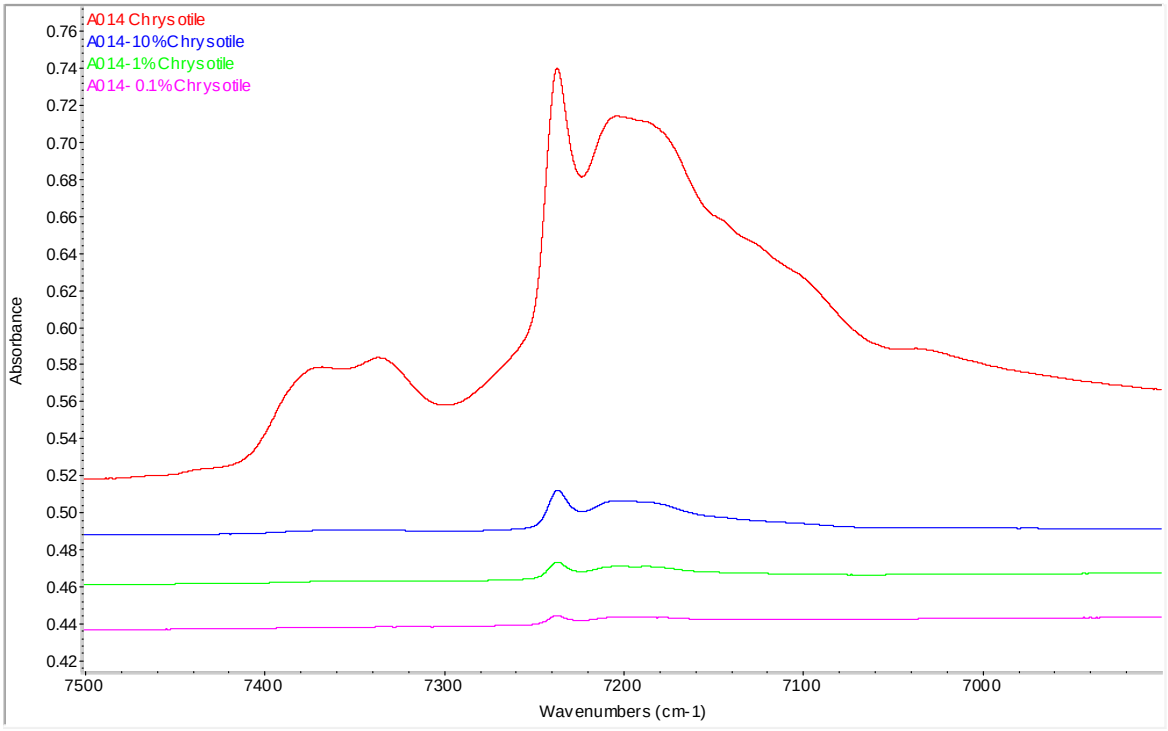

Figure S11a. NIR spectra of chrysotile in $CaCO_3$: different concentration (resolution = 2 cm^{-1}). Common scale option, spectra are offset for clarity.

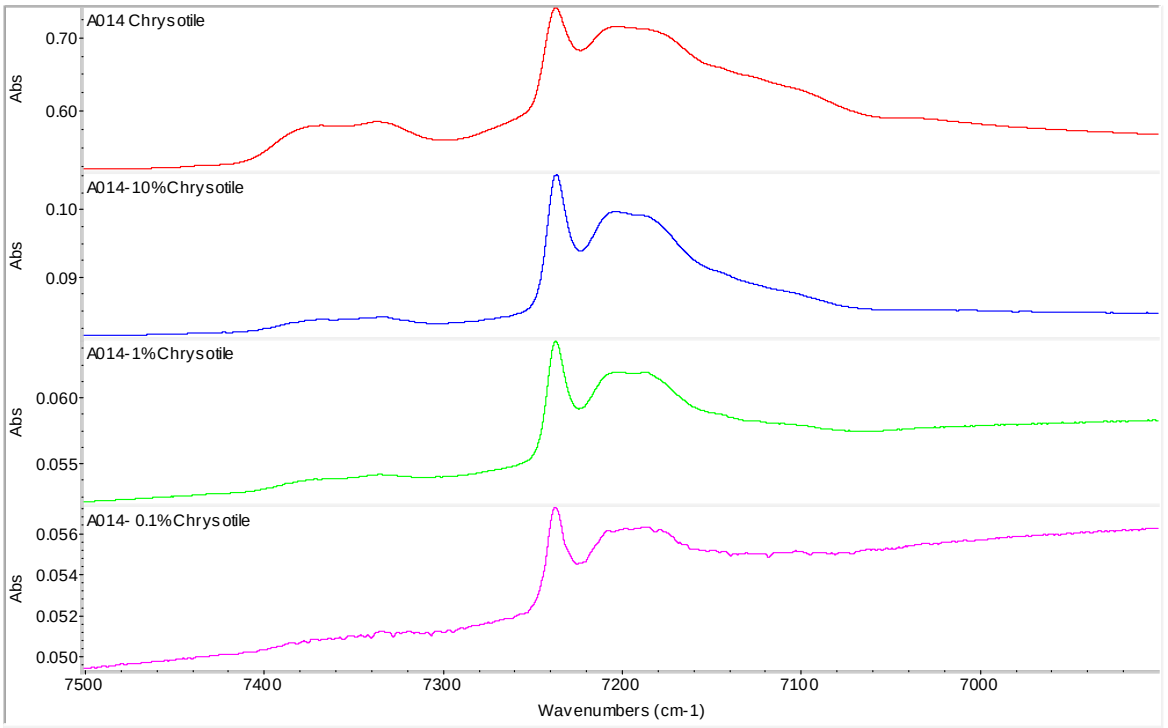

Figure S11b. NIR spectra of chrysotile in $CaCO_3$: different concentration (resolution = 2 cm^{-1}). Full scale option to demonstrate the high signal to noise ratio.

153

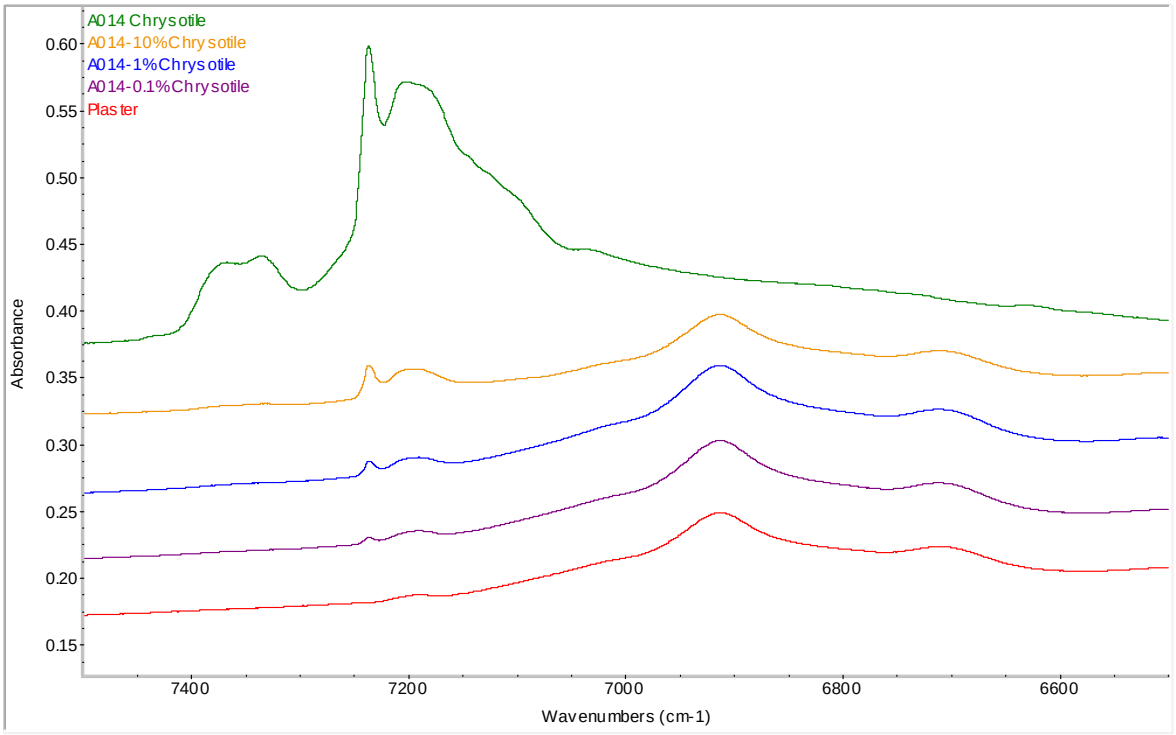

Figure S11c. NIR spectra of chrysotile in plaster: different concentration (resolution = 2 cm^{-1}). Common scale option, spectra are offset for clarity.

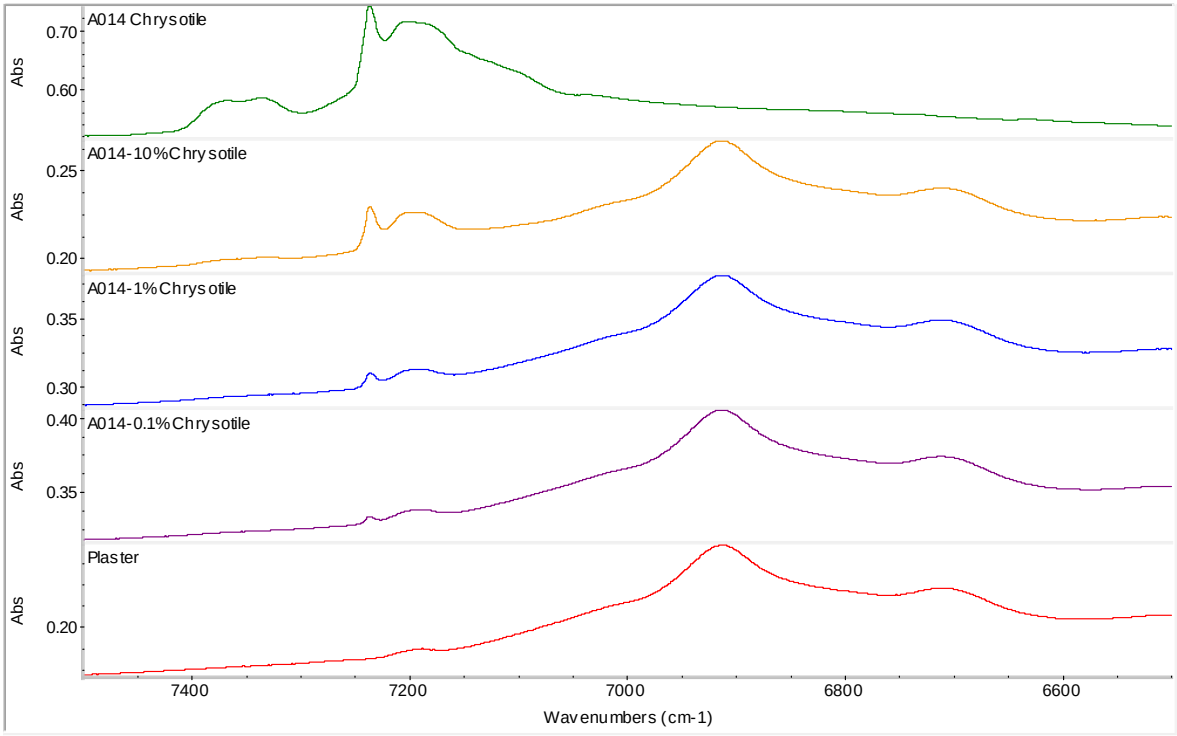

Figure S11d. NIR spectra of chrysotile in plaster: different concentration (resolution = 2 cm^{-1}). Full scale option to demonstrate the high signal to noise ratio.

154

155

156

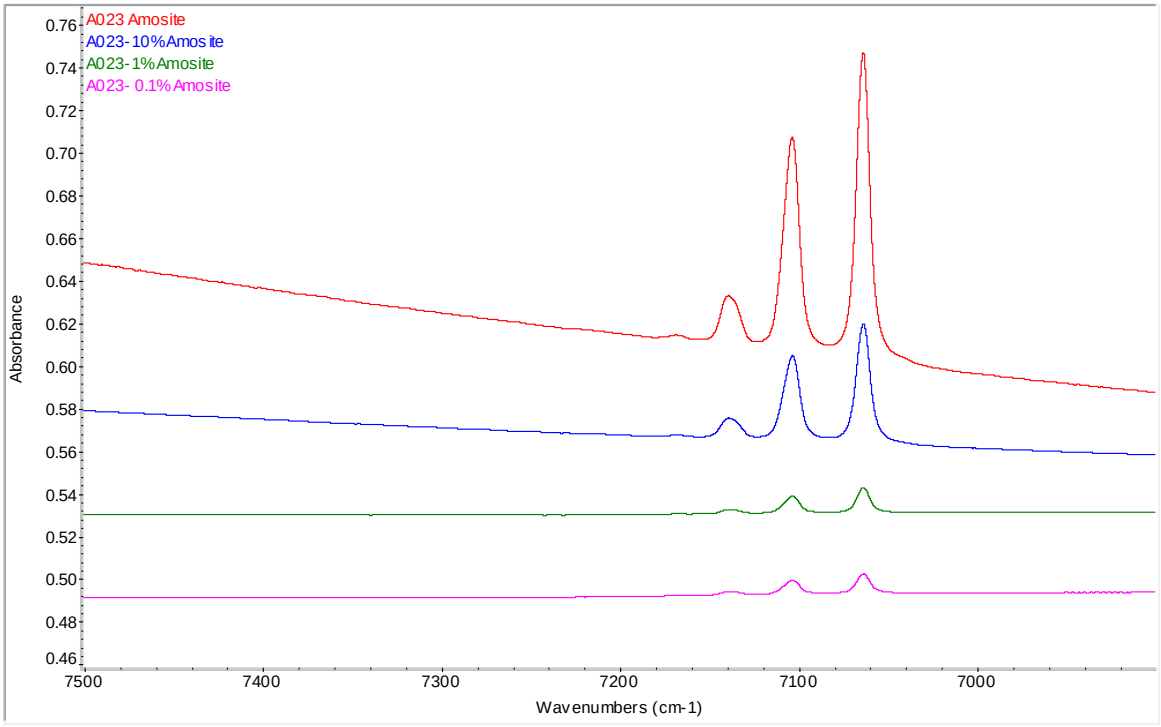

Figure S11e. NIR spectra of amosite in $CaCO_3$: different concentration (resolution = 2 cm^{-1}). Common scale option, spectra are offset for clarity.

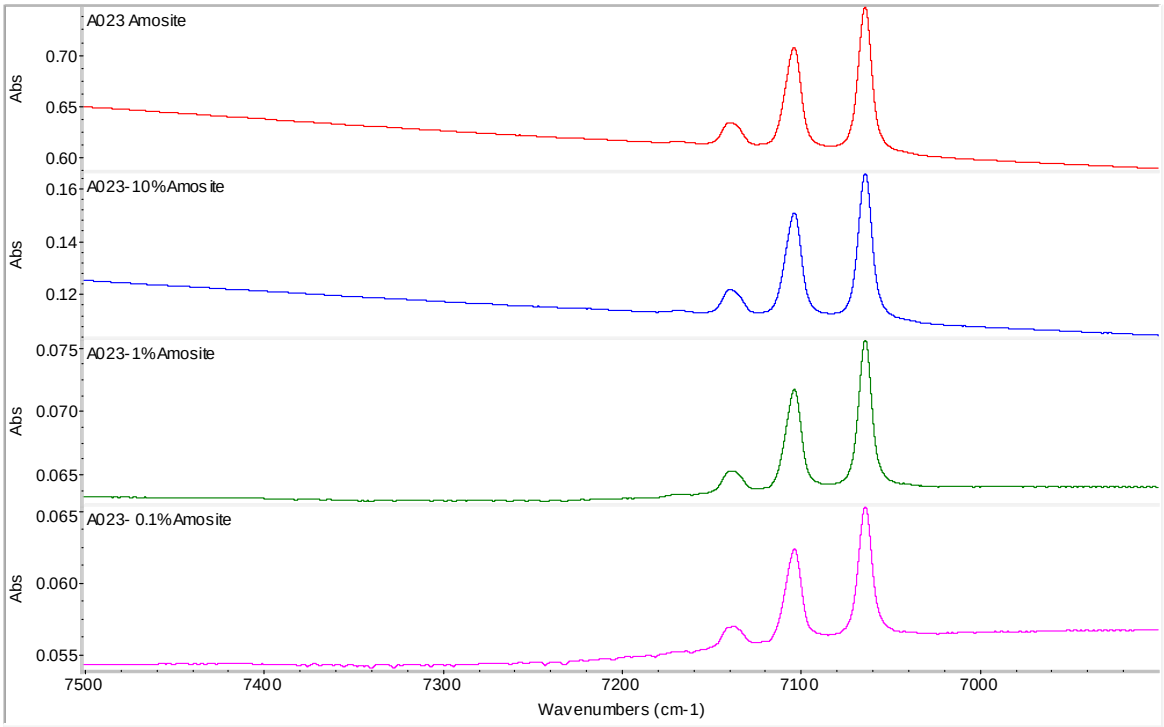

Figure S11f. NIR spectra of amosite in $CaCO_3$: different concentration (resolution = 2 cm^{-1}). Full scale option to demonstrate the high signal to noise ratio.

157

158

159

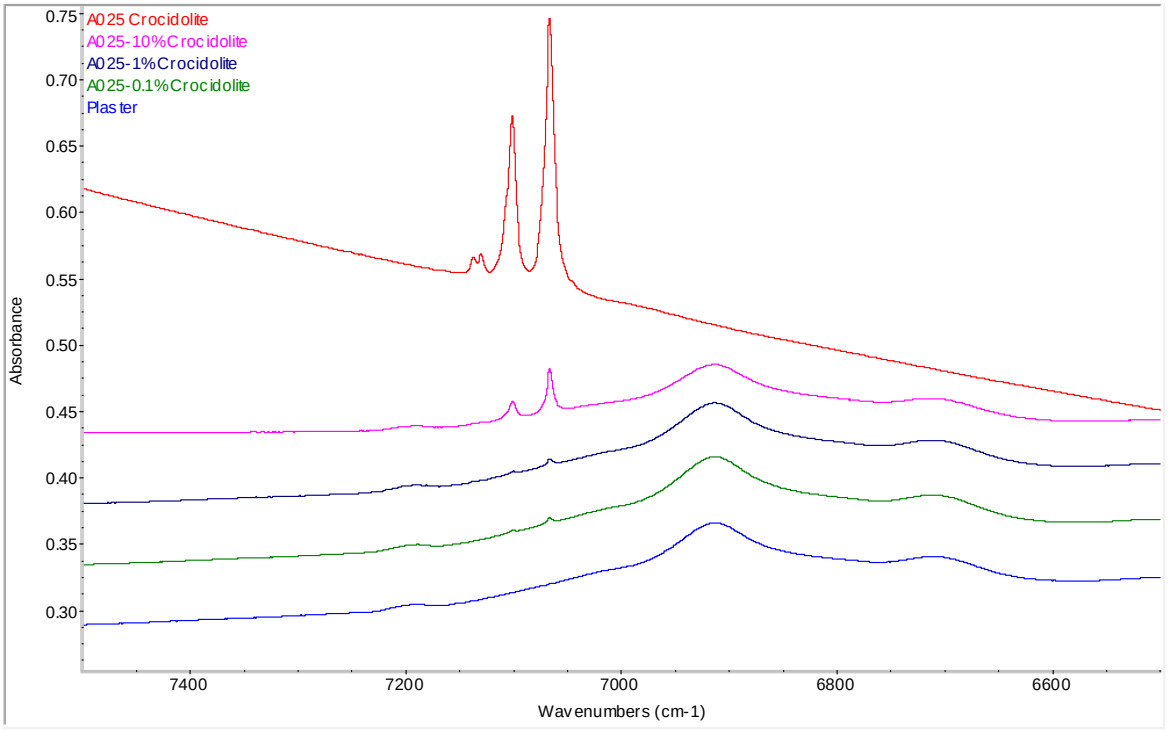

Figure S11g. NIR spectra of crocidolite in plaster: different concentration (resolution = 2 cm^{-1}). Common scale option, spectra are offset for clarity.

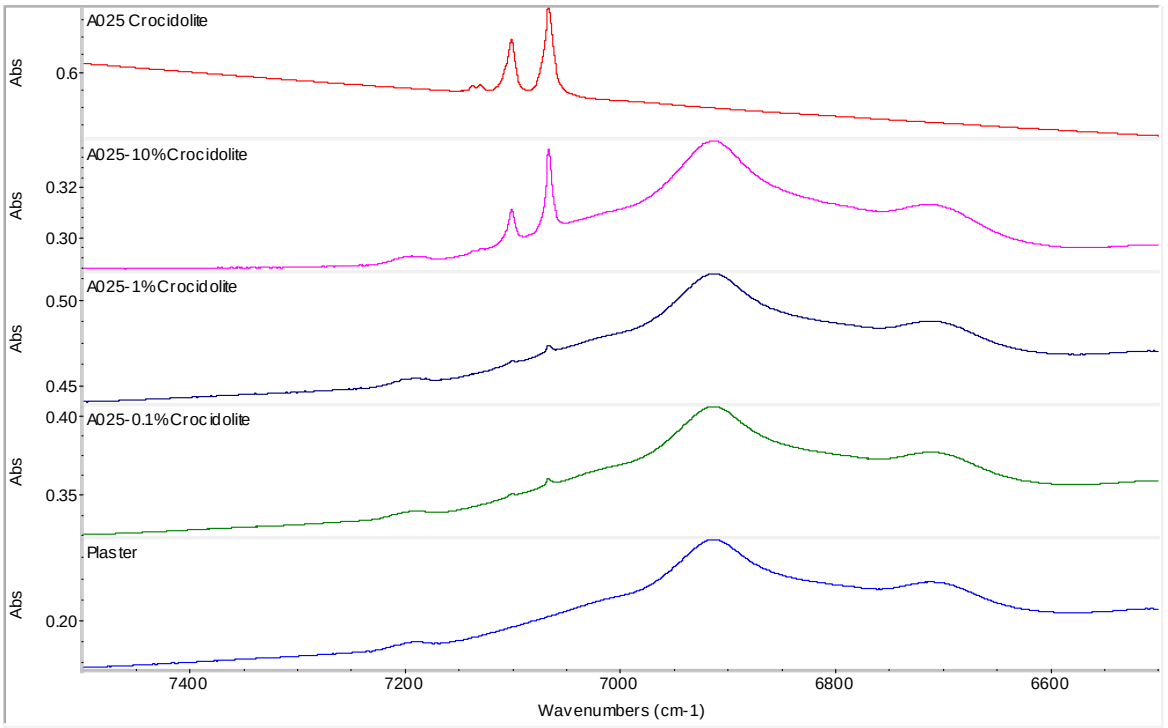

Figure S11h. NIR spectra of crocidolite in plaster: different concentration (resolution = 2 cm^{-1}). Full scale option to demonstrate the high signal to noise ratio.

160

161

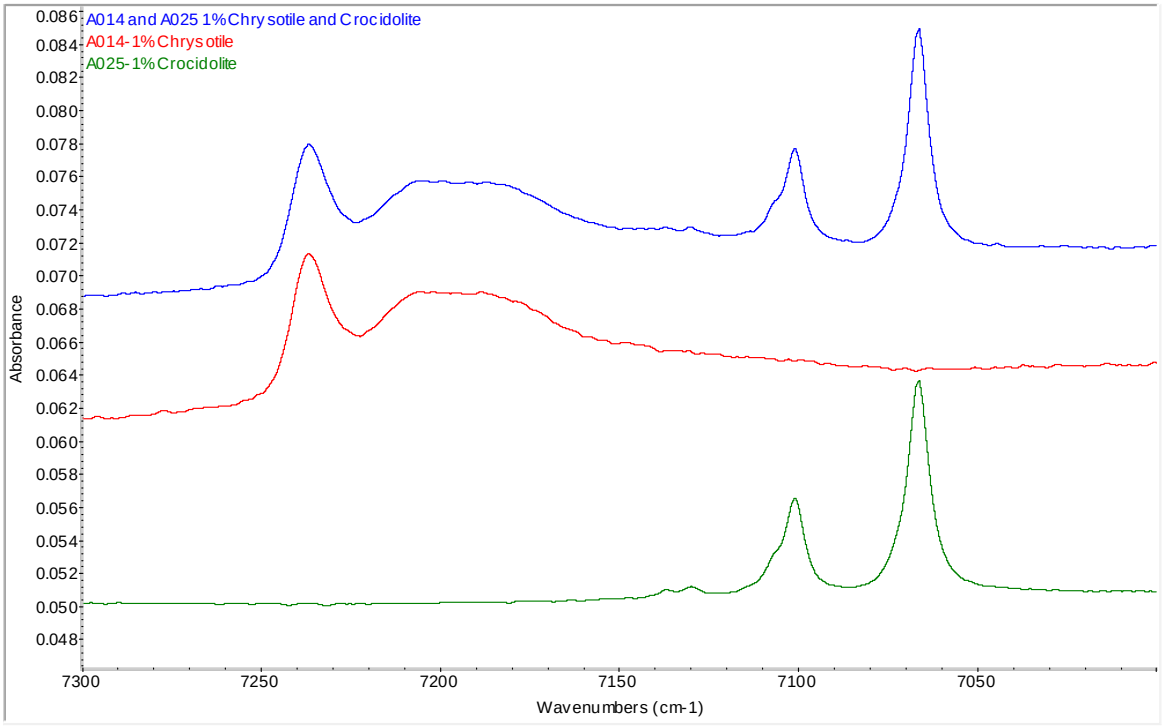

Figure S12a. NIR spectra of asbestos mixtures: crocidolite and chrysotile (resolution = 2 cm^{-1}). Common scale option, spectra are offset for clarity.

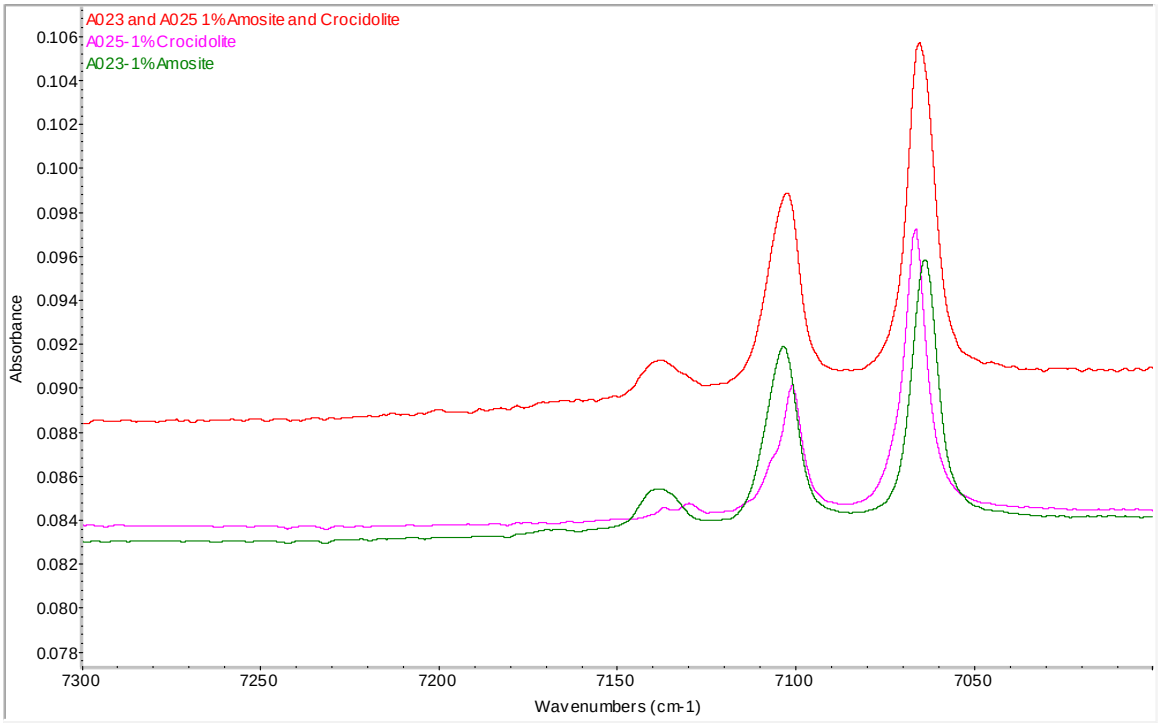

Figure S12b. NIR spectra of asbestos mixtures: (resolution = 2 cm^{-1}). Common scale option, spectra are offset for clarity.

165

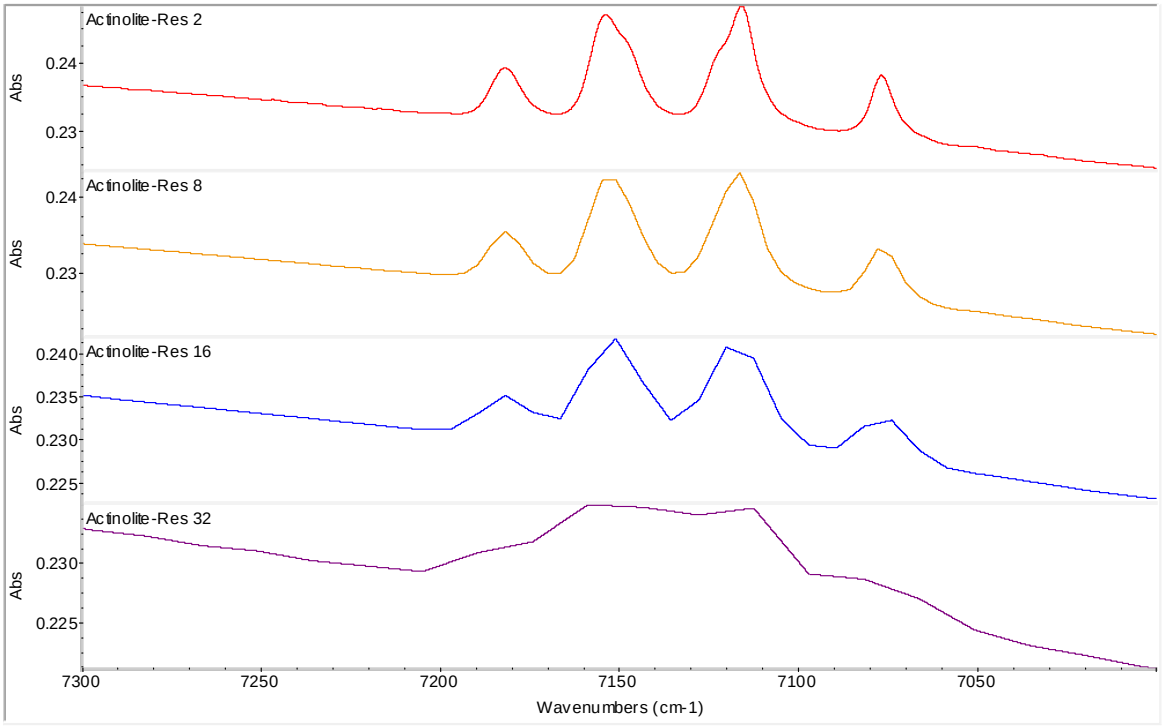

Figure S13a. NIR spectra of actinolite collected at different resolution.

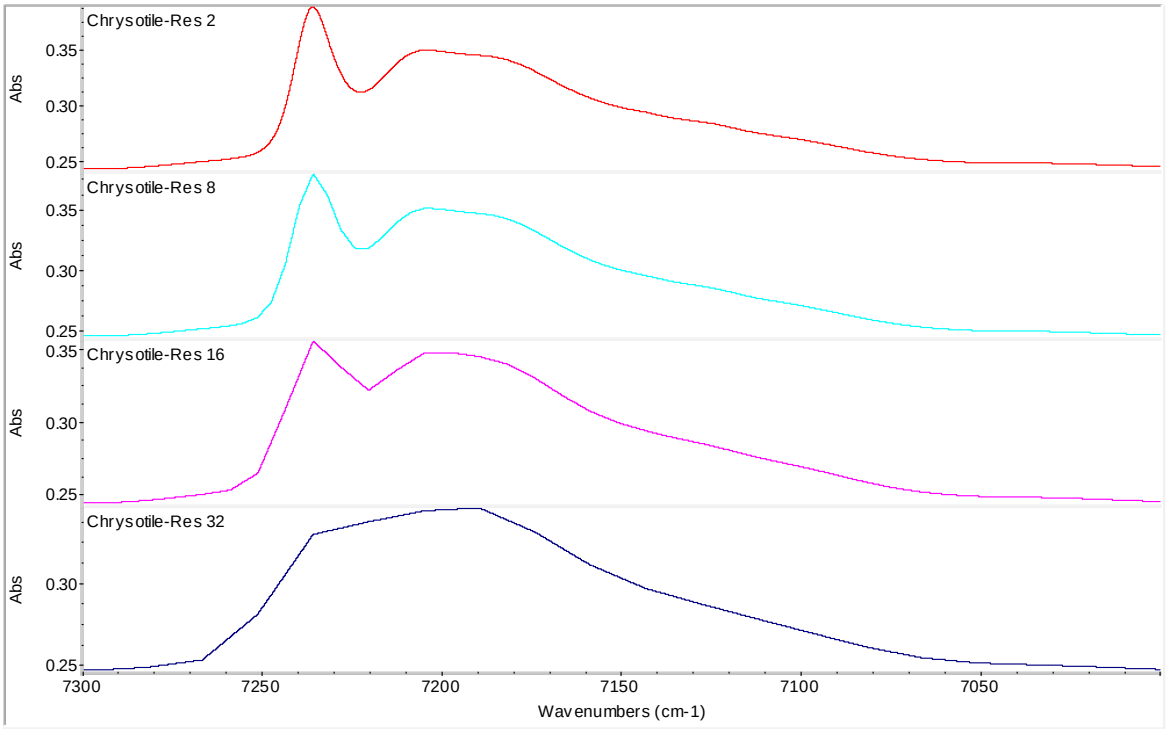

Figure S13b. NIR spectra of chrysotile collected at different resolution.

166

167

168

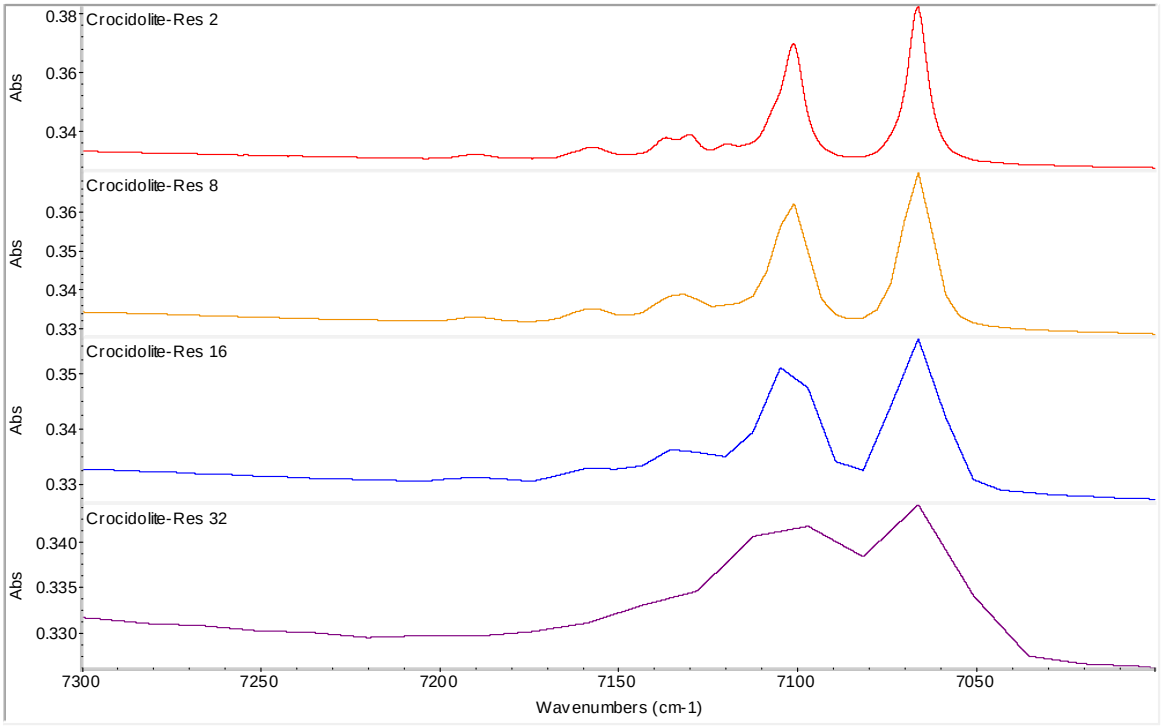

Figure S13c. NIR spectra of crocidolite collected at different resolution.

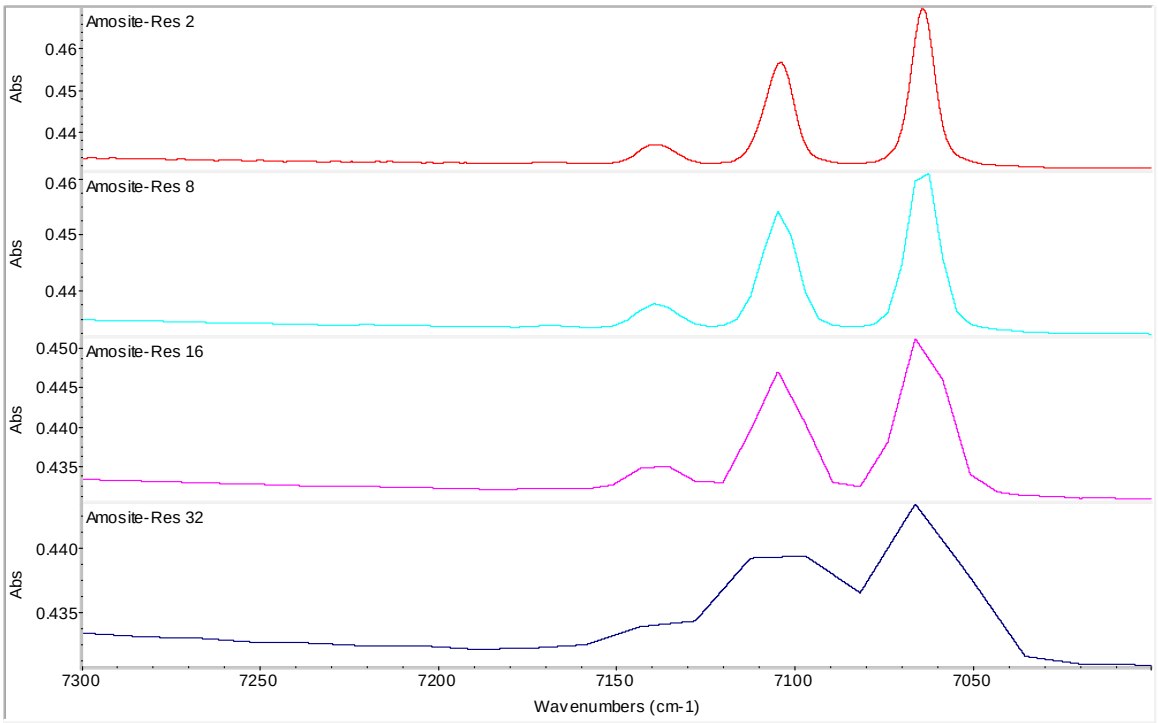

Figure S13d. NIR spectra of amosite collected at different resolution.

169

170

171

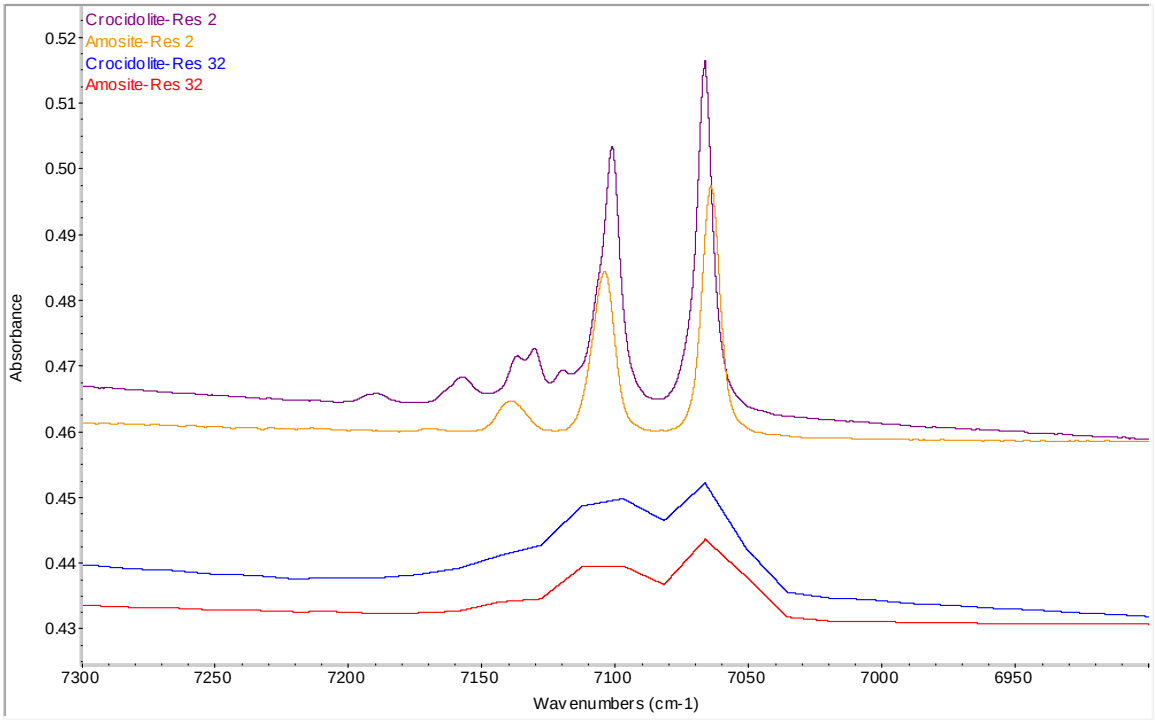

Figure S13e. NIR spectra of crocidolite and amosite collected at different resolution. Common scale option, spectra are offset for clarity.

172

173

A list of 50 samples presented Table S5, including reference materials and ACM, which have been used for the NIR examination and following analysis of the data by the Asbestos-Tester-4 program. (TRUE indicates the presence of asbestos according to PLM and FTIR data.)

Table S5. Samples utilised for the computational testing of the NIR data.

	Sample	Description	actinolite	amosite	anthophyllite	chrysotile	crocidolite	tremolite	Colour
1	HSL standard	chrysotile				TRUE			light
2	HSL standard	tremolite						TRUE	light
3	HSL standard	actinolite	TRUE						light
4	HSL standard	amosite		TRUE					light
5	HSL standard	crocidolite					TRUE		light
6	HSL standard	anthophyllite			TRUE				light
7	Geo standard	tremolite						TRUE	dark
8	Geo standard	actinolite	TRUE						dark
9	Geo standard	chrysotile				TRUE			light
10	Geo standard	crocidolite					TRUE		dark
11	Geo standard	anthophyllite			TRUE				dark
12	Geo standard	amosite		TRUE					dark
13	CaCO3 mix	crocidolite 10%					TRUE		light
14	CaCO3 mix	amosite 10%		TRUE					light
15	CaCO3 mix	chrysotile 10%				TRUE			light
16	Unknown	tile				TRUE			light
17	Unknown	pipe lagging				TRUE			light
18	Unknown	insulation				TRUE			light
19	Unknown	tile+bitumen				TRUE			light
20	Unknown	plaster					TRUE		light
21	Unknown	plaster		TRUE					light
22	Unknown	cement					TRUE		light
23	Unknown	cement					TRUE		dark
24	Unknown	felt+bitumen							light
25	Unknown	wet lagging					TRUE		light
26	Unknown	mortar			TRUE				light
27	Unknown	cement							light
28	Unknown	debris							light
29	Unknown	plaster							light
30	Unknown	sepiolite						TRUE	light
31	Unknown	paint		TRUE					light
32	Unknown	plaster		TRUE					light
33	Unknown	vermiculate	TRUE					TRUE	light
34	Unknown	plaster				TRUE			light
35	Unknown	plaster							light
36	Unknown	tile				TRUE			light
37	Unknown	insulation			TRUE	TRUE			light
38	Unknown	grout							dark
39	Unknown	chalk			TRUE				light
40	Unknown	cement		TRUE		TRUE			light
41	Unknown	boarding		TRUE		TRUE			light
42	Unknown	textured coating			TRUE				light
43	Martrix	plaster							light
44	Martrix	plasterboard							light
45	Martrix	cement							light
46	Martrix	artex powder							light
47	Martrix	insulation wool							light
48	CaCO3 mix	chrysotile+crocidolite				TRUE	TRUE		light
49	CaCO3 mix	amosite+crocidolite			TRUE		TRUE		light
50	CaCO3 mix	amosite+chrysotile			TRUE	TRUE			light

Table S6 presents a selection of the final outputs (a complete set is included in SI as a csv file), which demonstrate very good agreement with the PLM and FTIR data on the composition of the questioned samples. At the same time, some variations are observed; these can be linked to different locations tested in the same sample and to some ACM most likely containing a mixture of amosite and crocidolite. In some cases, NIR spectroscopy appears to be more sensitive than PLM and mid-range FTIR.

Table S6. A selection of the computational analysis results.

Sample	actinolite	amosite	chrysotile	crocidolite
Sample16_1.CSV	FALSE	FALSE	TRUE	FALSE
Sample16_2.CSV	FALSE	FALSE	TRUE	FALSE
Sample16_3.CSV	FALSE	FALSE	TRUE	FALSE
Sample16_4.CSV	FALSE	FALSE	TRUE	FALSE
Sample16_5.CSV	FALSE	FALSE	TRUE	FALSE
Sample16_6.CSV	FALSE	FALSE	TRUE	FALSE
Sample16_7.CSV	FALSE	FALSE	TRUE	FALSE
Sample16_8.CSV	FALSE	FALSE	TRUE	FALSE
Sample16_9.CSV	FALSE	FALSE	TRUE	FALSE
Sample17_1.CSV	FALSE	FALSE	TRUE	FALSE
Sample17_2.CSV	FALSE	FALSE	TRUE	FALSE
Sample17_3.CSV	FALSE	FALSE	TRUE	FALSE
Sample17_4.CSV	FALSE	FALSE	TRUE	FALSE
Sample17_5.CSV	FALSE	FALSE	TRUE	FALSE
Sample17_6.CSV	FALSE	FALSE	TRUE	FALSE
Sample17_7.CSV	FALSE	FALSE	TRUE	FALSE
Sample17_8.CSV	FALSE	FALSE	TRUE	FALSE
Sample17_9.CSV	FALSE	FALSE	TRUE	FALSE
Sample18_1.CSV	FALSE	FALSE	TRUE	FALSE
Sample18_2.CSV	FALSE	FALSE	TRUE	FALSE
Sample18_3.CSV	FALSE	FALSE	TRUE	FALSE
Sample18_4.CSV	FALSE	FALSE	TRUE	FALSE
Sample18_5.CSV	FALSE	FALSE	TRUE	FALSE
Sample18_6.CSV	FALSE	FALSE	TRUE	FALSE
Sample18_7.CSV	FALSE	FALSE	TRUE	FALSE
Sample18_8.CSV	FALSE	FALSE	TRUE	FALSE
Sample18_9.CSV	FALSE	FALSE	TRUE	FALSE

Sample	actinolite	amosite	chrysotile	crocidolite
Sample19_1.CSV	FALSE	TRUE	TRUE	FALSE
Sample19_2.CSV	FALSE	TRUE	TRUE	TRUE
Sample19_3.CSV	FALSE	FALSE	TRUE	FALSE
Sample19_4.CSV	FALSE	FALSE	TRUE	FALSE
Sample19_5.CSV	FALSE	FALSE	TRUE	FALSE
Sample19_6.CSV	FALSE	FALSE	TRUE	FALSE
Sample19_7.CSV	FALSE	TRUE	TRUE	FALSE
Sample19_8.CSV	FALSE	TRUE	TRUE	FALSE
Sample19_9.CSV	FALSE	TRUE	TRUE	FALSE
Sample20_1.CSV	FALSE	FALSE	FALSE	TRUE
Sample20_2.CSV	FALSE	FALSE	FALSE	TRUE
Sample20_3.CSV	FALSE	FALSE	FALSE	TRUE
Sample20_4.CSV	FALSE	FALSE	FALSE	TRUE
Sample20_5.CSV	FALSE	FALSE	FALSE	TRUE
Sample20_6.CSV	FALSE	FALSE	FALSE	TRUE
Sample20_7.CSV	FALSE	FALSE	FALSE	TRUE
Sample20_8.CSV	FALSE	FALSE	FALSE	TRUE
Sample20_9.CSV	FALSE	FALSE	FALSE	TRUE
Sample21_1.CSV	FALSE	TRUE	FALSE	FALSE
Sample21_2.CSV	FALSE	TRUE	FALSE	FALSE
Sample21_3.CSV	FALSE	TRUE	FALSE	FALSE
Sample21_4.CSV	FALSE	TRUE	FALSE	TRUE
Sample21_5.CSV	FALSE	TRUE	FALSE	TRUE
Sample21_6.CSV	FALSE	TRUE	FALSE	TRUE
Sample21_7.CSV	FALSE	TRUE	FALSE	FALSE
Sample21_8.CSV	FALSE	TRUE	FALSE	FALSE
Sample21_9.CSV	FALSE	TRUE	FALSE	FALSE

References

1 A. Marconi, *Application of infrared spectroscopy in asbestos mineral analysis*. Annali dell Istituto Superiore di Satina, **1983**, 19, 629-638.

2 I.R. Lewis, N.C. Chaffin, M.E. Gunter, P.R. Griffiths, *Vibrational spectroscopic studies of asbestos and comparison of suitability for remote analysis,* Spectrochimica Acta A, **1996,** 52, 315-328.

3 E. Foresti, M. Gazzano, A.F. Gualtieri, I.G. Lesci, B. Lunelli, G. Pecchini, E. Renna, N. Roveri, *Determination of low levels of free fibres of chrysotile in contaminated soils by X-ray diffraction and FTIR spectroscopy*. Analytical and Bioanalytical Chemistry, **2003**, 376, 653-658.

4 V. Sontevska, G. Jovanovski, P. Makreski, *Minerals from Macedonia. Part XIX. Vibrational spectroscopy as identificational tool for some sheet silicate minerals*. Journal of Molecular Structure, **2007**, 834-836, 318-327.

5 E. Foresti, E Fornero, I.G. Lesci, C Rinaudo, T. Zuccheri, N. Roveri. *Asbestos health hazard: A spectroscopic study of synthetic geoinspired Fe-doped chrysotile,* Journal of Hazardous Materials, **2009**, 167, 1070-1079.

6 M. Sitarz, W. Jastrzňbski, P. JeleŒ, E. DğıgoŒ, M. Gawňda, *Preparation and structural studies of black glasses based on ladder-like silsesquioxanes*. Spectrochimica Acta Part A: Molecular and Biomolecular Spectroscopy, **2014**, 132, 884-888.

7 M. Sitarz, W. Mozgawa, M. Handke, *Vibrational spectra of complex ring silicate anions - method of recognition.* J. Molecular Structure, **1997**, 404, 193-197.

8 C. Rinaudo, E. Belluso, D. Gastaldi. *Assessment of the use of Raman spectroscopy for the determination of amphibole asbestos,* Mineralogical Magazine, **2004**, 68, 455-465.

9 C. Rinaudo, D. Gastaldi, E. Belluso. *Characterization of chrysotile, antigorite and lizardite by FT-Raman spectroscopy,* Canadian Mineralogist, **2003**, 41, 883-890.

10 D. Bard, B. Tylee, K. Williams, J. Yarwood. *Use of a fibre-optic probe for the identification of asbestos fibres in bulk materials by Raman spectroscopy*, Journal of Raman Spectroscopy, **2004**, 35, 541-548.

11 A. Bloise, E. Fornero, D. Gastaldi, E. Belluso, E. Barrese, C. Rinaudo. *Synthesis and characterization of tremolite asbestos fibres*, European Journal of Mineralogy, **2008**, 20, 1027-1033.

12 J.T. Kloprogge, R.L. Frost, L. Rintoul, *Single crystal Raman microscopic study of the asbestos mineral chrysotile*, Phys. Chem. Chem. Phys., **1999**, 1, 2559-2564.

13 J. Jehlicka, P. Vítek, H.G.M. Edwards, M. Heagraves, T. Capoun. *Application of portable Raman instruments for fast and non-destructive detection of minerals on outcrops*, Spectrochimica Acta Part A, **2009**, 73, 410-419.

14 R. Petry, R. Mastalerz, S. Zahn, T.G. Mayerhçfer, G. Volksch, L. Viereck-Gotte, B. Kreher-Hartmann, L. Holz, M. Lankers, J. Popp. *Asbestos mineral analysis by UV Raman and energy-dispersive x-ray spectroscopy*, ChemPhysChem, **2006**, 7, 414-420.